REVISTAMATĒRIA
V.29 N.2
ISSN 1517-7076 Articles e20240075, 2024

Thermal analysis of modified segmented switched reluctance motor with aluminium metal matrix composite fins used in cooling fan applications

Augustine Mathu Gnaniah[1], Fantin Irudaya Raj Edward Sehar*[2], Appadurai Mangalaraj[3], Balaji Mahadevan[4]

[1]Loyola-ICAM College of Engineering and Technology, Department of Electrical and Electronics Engineering. Tamil Nadu, India.

[2]Dr. Sivanthi Aditanar College of Engineering, Department of Electrical and Electronics Engineering. Tamil Nadu, India.

[3]Nehru College of Engineering and Research Centre, Department of Mechanical Engineering. Kerala, India.

[4]Sri Sivasubramaniya Nadar College of Engineering, Department of Electrical and Electronics Engineering. Tamil Nadu, India.

e-mail: gnanaugus@gmail.com, fantinraj@gmail.com, appadurai86@gmail.com, balajim@ssn.edu.in

ABSTRACT

The switched reluctance motor (SRM) plays a significant role in many industrial applications. Among the various topologies of SRM, modified segmented rotor SRM (MSRSRM) overcomes the shortfalls of conventional SRM. From an application perspective, the analysis of electromagnetic and thermal aspects of segmented rotor SRM becomes crucial. In the present work, the thermal analysis for modified segmented rotor SRM used in cooling fan applications is detailed. The effect of temperature rises in the different parts of the machine due to electromagnetic losses is identified by using the finite element software package ANSYS. External fin-based convective cooling strategy is adopted and analysed for the MSRSRM proposed in the present work. Choosing the suitable fin material and arrangements of fins play a crucial role in the effective thermal management of the MSRSRM. Three different Aluminium (Al) Metal Matrix Composites (MMC) based fins are considered for this analysis. In addition, the optimum number of fins and their thickness are also identified using thermal analysis. The results revealed that the Al/Diamond MMC-based fins are more effective compared with other fin materials. Also, the axial type-thin fin (1mm) arrangement yields better results compared with other fin arrangements.

Keywords: Modified Segmented rotor SRM; Thermal Analysis; Fins; Natural Convection; Thermal Management System.

1. INTRODUCTION

In recent years researchers have been actively exploring Switched Reluctance Motors (SRM) for variable speed applications like traction, electric vehicles, aerospace, and domestic & industrial utilities. The major factors like rugged structure, simplicity, and inherent fault-tolerant capabilities encourage the industrial application of SRM [1–4]. By evolving novel structures and control strategies the SRM has become a competitor to the PM-assisted machines [5–8]. The SRM configuration with discrete segments in the rotor provides an improvement in efficiency compared with the conventional SRM [9]. The stator with an E-core shape results in the free flux reversal and reduces the core losses predominantly by reducing the hysteresis loss [10]. These types of structural modifications in the rotor and stator significantly improve the mechanical power output and overall efficiency. In addition, it will minimize the acoustic noise [11].

The sensitivity parameters in design considerations like pole arc variations, tapered stator pole, and non-uniform air gap between the stator pole face and rotor pole shoe show significant improvement in the performance of the motor [12]. The novel rotor structure with flux reversal free stator has been proposed to improve electrical utilization and to provide higher torque density. Predicting a design configuration's performance and comparing it with the existing topologies electromagnetic analysis plays a significant role in machine design. The electromagnetic analysis of the segmented rotor with excited and auxiliary poles and the influence of laminating material on performance enhancement have been detailed in the literature [13, 14]. Apart from electromagnetic characteristics, thermal behaviour is a major factor that influences the performance of SRM. The effect of thermal stress due to the failure of insulation has been discussed by [15, 16]. Temperature

Corresponding Author: E. Fantin Irudaya Raj Received on 26/02/2024 Accepted on 19/03/2024

DOI: https://doi.org/10.1590/1517-7076-RMAT-2024-0075

rise estimation explores the life span of the windings and insulation of laminating materials. The Computational Fluid dynamics (CFD), Thermal Finite Element Analysis (FEA) techniques, and coupled circuit model approaches have been suggested by the authors to predict the temperature distribution in electrical machines [17–22]. The current work explores the thermal behaviour of the novel modified segmented rotor type SRM (MSRSRM) and aims to propose suitable cooling arrangements.

There are different types of cooling strategies proposed for efficient thermal management of electrical machines in the literature [23, 24]. Among the proposed methodologies, convective heat transfer using fin arrangements plays a vital role. External fin configurations come in various shapes and sizes, described in-depth in the literature. Choosing a suitable fin material and type of fin arrangement plays a crucial role in the effective thermal management of the SRM. There are numerous materials used for such applications reported in the literature [25–30]. Among these Aluminium metal matrix composite materials have attracted more interest in recent times. From the literature, it is also evident that a comprehensive analysis from electromagnetic and thermal aspects becomes imperative from the application perspective of these novel MSRSRM configurations. The main goal of this study is to find the best fin arrangement for a segmented rotor SRM to reduce temperature rise. Furthermore, the optimal number of fins and fin height is determined for the motor understudy.

2. ELECTROMAGNETIC ANALYSIS OF MODIFIED 6/5 SEGMENTED ROTOR SRM

The objective of the electromagnetic analysis is to analyze the behavior of the SRM by understanding the interactions between magnetic fields, electrical currents, and mechanical motion. From the elementary equivalent circuit, the fundamental voltage equation for an SRM will be defined by neglecting the mutual inductance. The per-phase voltage equation of the proposed SRM configuration is given in Equation 1.

$$V = i_s R_s + \frac{d\lambda(\theta, i_s)}{dt} \tag{1}$$

Where R_s is per phase stator resistance in ohms, i_s is per phase stator current in amps, λ is per phase flux linkage in wb-turn and θ is position of the rotor in deg.

The amount of flux linked with the core for the given proposed 6/5 MSSRM is represented in equation 2,

$$\lambda = L(\theta, i_s)\, i_s \tag{2}$$

where, L is inductance per phase which depends on the position of the rotor and phase current. The voltage equation for 6/5 MSSRM can be written in equation 3–5.,

$$V = R_s i_s + \frac{d[L(\theta, i_s)\, i_s]}{dt} \tag{3}$$

$$V = R_s i_s + L(\theta, i_s)\frac{di_s}{dt} + i_s \frac{d\theta}{dt}\frac{d\{L(\theta, i_s)\}}{d\theta} \tag{4}$$

$$V = R_s i_s + L(\theta, i_s)\frac{di_s}{dt} + \frac{dL(\theta, i_s)}{d\theta}\omega_m i_s \tag{5}$$

where $\omega_m = \dfrac{d\theta}{dt}$

The air gap power (P_{ag}) developed in the motor is given in equation 6 and equation 7.

$$P_{ag} = \frac{1}{2} i_s^2 \frac{dL(\theta, i_s)}{dt} = \frac{1}{2} i_s^2 \frac{dL(\theta, i_s)}{d\theta}\frac{d\theta}{dt} \tag{6}$$

$$P_{ag} = \frac{1}{2} i_s^2 \frac{dL(\theta, i_s)}{d\theta}\omega_m \tag{7}$$

The major contribution in the development of mechanical power in the rotor is contributed by the airgap power. The developed mechanical rotor power equation is given in equation 8.

$$P_m = \omega_m T_m \tag{8}$$

Where ω_m is the angular speed of the motor, T_m is torque developed by the motor.

By equating the above equations (6) & (7) the developed motor torque equation is obtained, and the developed motor torque equation is represented in equation 9.

$$T_m = \frac{1}{2} i_s^2 \frac{dL(\theta, i_s)}{d\theta} \tag{9}$$

The average torque produced by the proposed MSSRM with respect to co energy is derived from the electromechanical energy conversion process. The derived average torque equation is given in equation 10.

$$T_{avg} = \frac{\left(W'_{f(al)} - W'_{f(ual)}\right)}{2\pi} mN_r \tag{10}$$

Where $W'_{f(al)}$ is the dissipated energy during aligned position; $W'_{f(ual)}$ is the amount of dissipated energy during unaligned position; m is number of phases; N_r is the number of rotor poles

The torque ripple of the 6/5 MSSRM is determined in the equation 11.

$$T_{ripple} = \frac{(T_{max} - T_{min})}{T_{max}} \tag{11}$$

where T_{max} is maximum torque available in the machine; T_{min} is minimum torque available in the machine.

The finite element analysis-based package is employed for the performance analysis of novel SRM structures [6]. A shorter flux path and flux reversal free stator structure have been considered for a 6/5 configuration. The flux reversal free SRM configuration improves the electrical energy utilization and magnetomotive force due to the provision of the shorter flux path [31–33]. The proposed configuration has 6 stator poles with excited poles and auxiliary poles. In the rotor, the proposed configuration has 5 rotor poles in segmented configuration.

The performance parameters like torque, torque ripple, and efficiency are predicted through the electromagnetic analysis for the proposed design configurations through the SIMCENTER MAGNET software package.

In [8], the comparison of various laminating materials and design modifications are introduced to the 6/5 segmented rotor SRM in order to improve the average torque and reduce the torque ripple. Figure 1 depicts the structure of modified 6/5 segmented rotor SRM. The design data for the 6/5 segmented rotor is tabulated in Table 1.

The performance analysis during the dynamic condition is shown in Figure 2. The comparative study of performance with respect to the initial design of 6/5 segmented rotor SRM is tabulated in Table 2. The results revealed that reduced torque ripple and improved efficiency can be achieved by modified 6/5 segmented rotor SRM. The modified 6/5 segmented rotor configuration led to a novel rotor configuration.

3. THERMAL ANALYSIS OF MODIFIED 6/5 SEGMENTED ROTOR SRM (MSRSRM)

In the field of industrial manufacturing technology, the usage of SRM motors is bound to increase. The high-power density and smaller heat dissipation area are the major advantages of SRM. The presence of excessive

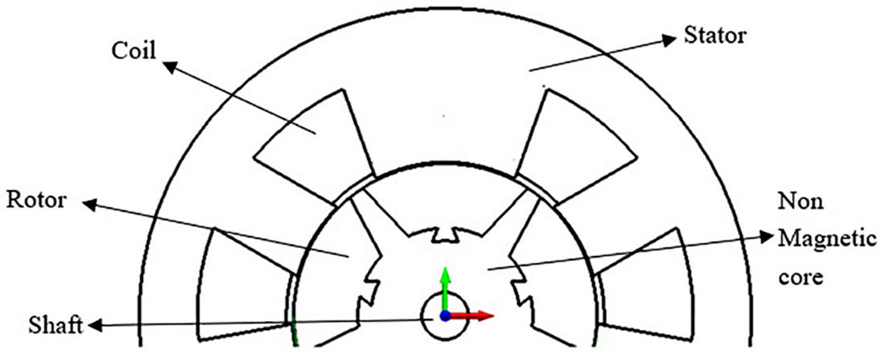

Figure 1: Structure of MSRSRM.

Table 1: Design date for Modified 6/5 segmented rotor SRM (MSRSRM).

PARAMETERS	SPECIFICATION
Number of stator main poles	3
Number of the auxiliary poles	3
Number of rotor poles	5
Power output (KW)	0.5
Voltage (V)	12
Current (A)	41.4
Turns per phase	26
Speed (rpm)	2800
Stator main pole arc	62
Stator auxiliary pole arc (deg)	30
Rotor pole arc (deg)	66
Outer stator diameter (mm)	105
Length of air gap (mm)	0.25
Shaft diameter (mm)	4
Stack length (mm)	35

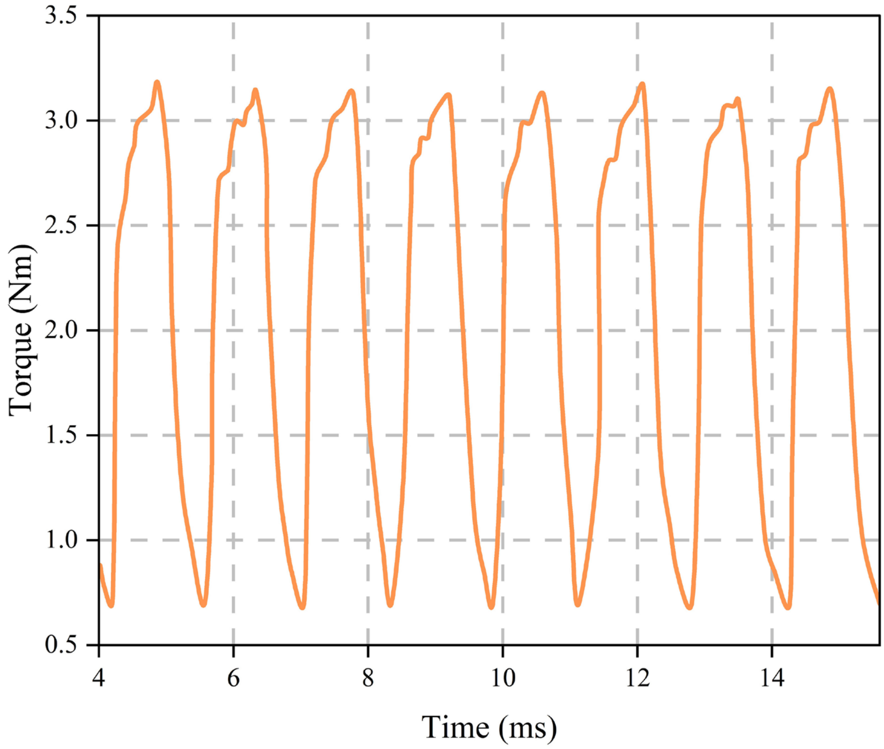

Figure 2: Dynamic torque characteristics of Modified 6/5 Segmented rotor SRM at rated conditions.

Table 2: Performance comparison.

PARAMETERS	TORQUE RIPPLE
12/8 Conventional SRM	1.504 p.u.
6/5 Segmented Rotor SRM	1.736 p.u.
Modified 6/5 Segmented Rotor SRM	1.525 p.u.

temperature rise blights the mechanical strength of the motor parts. The rise in the temperature tends to reduce the performance of the electrical machines through the deterioration of insulation [15, 22]. Since the life span of insulation materials in winding and lamination relies on the temperature rise. The analysis of temperature rise during the design process of SRM is required to suggest appropriate thermal cooling. In this paper, numerical approach techniques are used to identify the temperature distribution through FEA.

3.1. Static analysis of MSRSRM

The total electric losses in the motor generate the heat and are used to investigate the distribution of temperature. In modified 6/5 segmented rotor SRM, the generated heat energy is transferred to the inner surface due to the turbulence in the air and by natural convection, the heat energy is transferred to the outer surface of the stator and air. The heat generated from the solid body to the air due to the presence of temperature difference is given as

$$Q = h_{cv}A(T - T_{air}) \quad (12)$$

Where Q represents the total amount of heat generated, h_{cv} represents the convection coefficient, A represents the total area. T represents the temperature of Modified 6/5 segmented rotor SRM, T_{air} represents atmospheric air temperature.

The steady-state thermal analysis for the MSRSRM is carried out using the ANSYS package. The convection coefficient is set as zero as the initial condition and the necessary data like the estimated generated heat value and the electrical load are applied to the elements in the model as an input. The distribution of temperature in different parts of the MSRSRM under steady state conditions is given in Figure 3.

3.2. Transient analysis of MSRSRM

The distribution of temperature in various parts of MSRSRM during transient conditions analyzed by performing transient analysis. The distribution of temperature in different parts of the MSRSRM under transient conditions is given in Figure 4. The reduction in electrical losses leads to the minimum temperature distribution in the stator. The comparative analysis of temperature distribution in the stator and rotor of MSRSRM is depicted in Figure 5. The distribution of temperature in different parts of the machine is tabulated in Table 3 as a comparative study. From the Table 3, it is evident that the temperature in the MSRSRM is increased by 7°C in the stator part and 6°C in the rotor part in comparison with conventional 12/8 SRM.

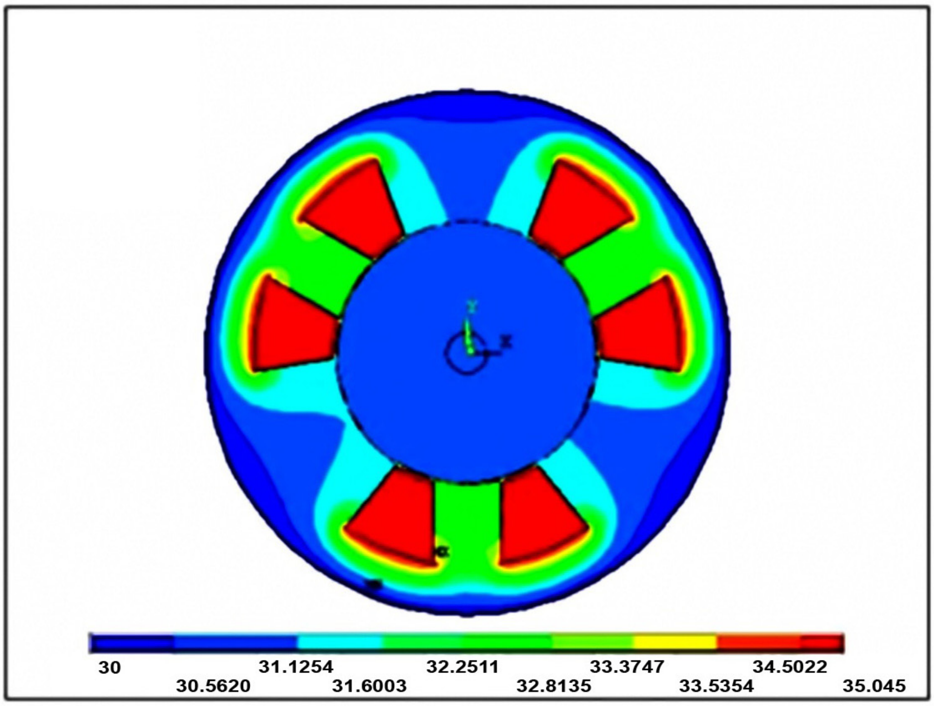

Figure 3: Distribution of temperature during steady state analysis of Modified 6/5 segmented rotor SRM.

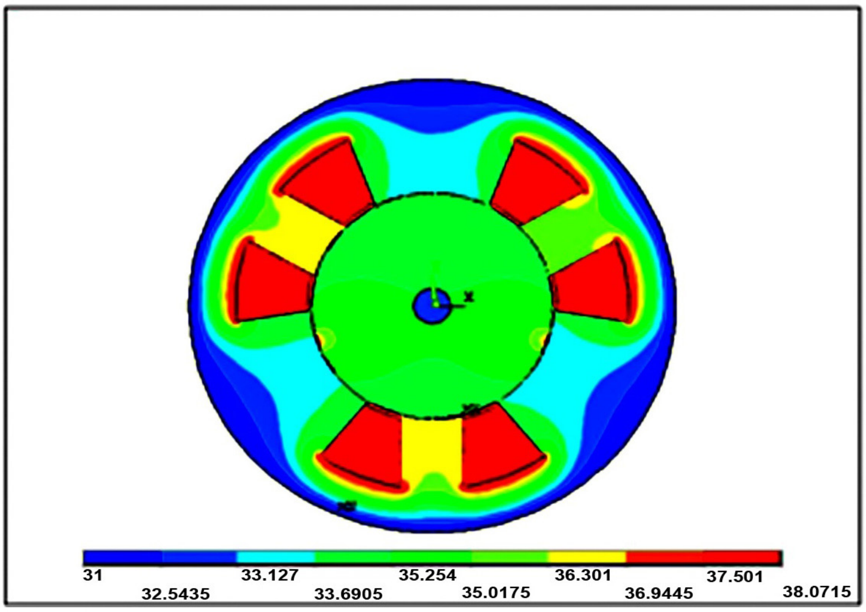

Figure 4: Distribution of temperature during transient analysis of Modified 6/5 segmented rotor SRM.

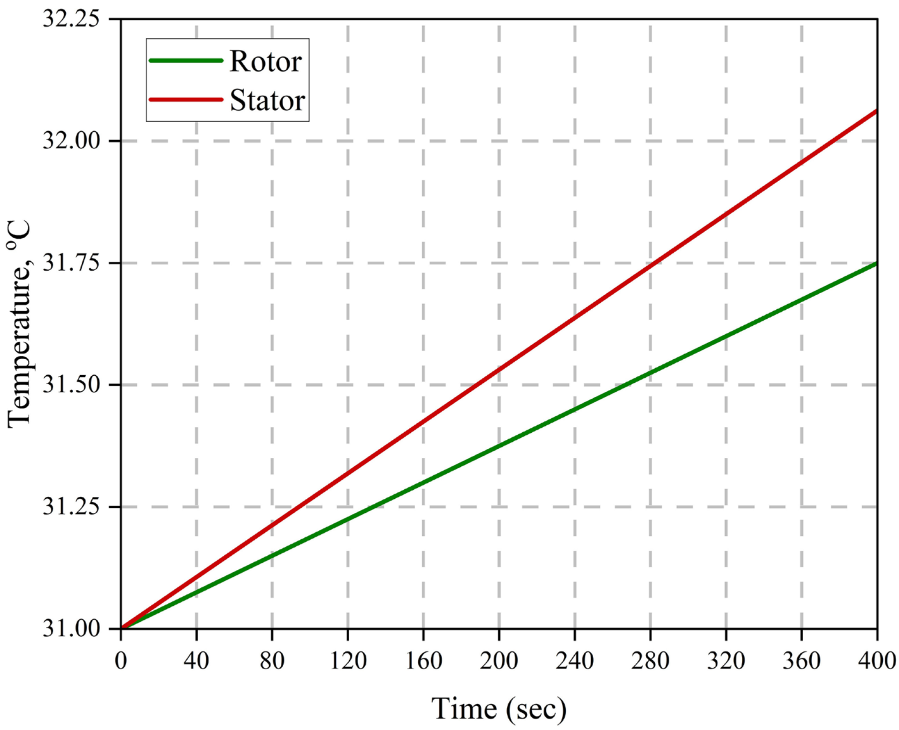

Figure 5: Variation of temperature rise in the stator and rotor region of MSRSRM.

Table 3: Comparison of temperature distribution in stator and rotor.

MACHINE TOPOLOGY	AVERAGE TEMPERATURE IN STATOR	AVERAGE TEMPERATURE IN THE ROTOR
12/8 SRM	24°C	26°C
Modified 6/5 segmented rotor SRM	31°C	32°C

4. MODELLING OF MODIFIED 6/5 SEGMENTED ROTOR SRM CASE

Through static and dynamic analysis of SRM, the temperature rise in the stator is found to be 31°C. The thermal energy is properly disposed of in the atmosphere through several conventional cooling techniques such as natural fin cooling, forced cooling systems integrated with fins, and water-cooling techniques. The forced and water-cooling technique is not required, since the temperature rise is very low. The natural fin cooling system is preferable to dissipate the waste heat energy due to energy losses. Several types of fin arrangement are available in the literature, among these axial and radial fin type majorly used in the electrical machines. And so, the axial and radial type types are required on the surface of the SRM to dissipate the thermal energy to atmosphere.

The axial fin and radial fin for the SRM are first modelled and then analysed in the ANSYS APDL module. The electric energy losses in the SRM are converted into heat energy. The waste heat energy in the rotor is transferred to the SRM surface through conductive heat transfer. The surface of the SRM must integrate with fins to transfer the waste heat from the SRM to the surroundings. The fins increase the contact surface area with the atmospheric air to enhance the convective heat transfer. The fins commonly made up of aluminium material for their better thermal conductivity. In this numerical analysis, different higher thermal conductivity aluminium (Al) metal matrix composite (MMC) materials are chosen for fin material. Since, the higher thermal conductivity material is added in the base metal for obtaining specific properties beyond the constituent materials. The materials chosen for the steady-state thermal analysis are given in Table 4. The radial and axial fin is analysed in the ANSYS solver to identify the effective material for fin configuration. Figure 6 shows the axial fin CATIA model and the Figure 7 shows the radial fin CATIA model. The CATIA fin model is imported into the ANSYS Workbench for steady state thermal analysis. The model is meshed first and then the boundary conditions for the thermal analysis are given. Here the quadratic type element is chosen for meshing and the element name is SOLID285. The mesh model of axial and radial fin arrangement is shown in Figure 8 and Figure 9 respectively. The thickness of the fin is taken as 1 mm, since the thin fins have effective heat transfer. The length of the fin is taken as 5 mm because the efficiency of the fin is decreased on higher fin length and mass of the fin is also increased.

Table 4: Fin material properties.

MATERIALS	THERMAL CONDUCTIVITY	DENSITY	SPECIFIC HEAT
Aluminium-Copper (Al/Cu) MMC	301 W/m K [34]	4578 kg/m^3	743.4 J/kg. K
Aluminium-Diamond (Al/Diamond) MMC	575 W/m K [35]	2943 kg/m^3	780.6 J/kg. K
Aluminium-Boron Nitride (Al/BN) MMC	475 W/m K [36]	2940 kg/m^3	882.9 J/kg. K

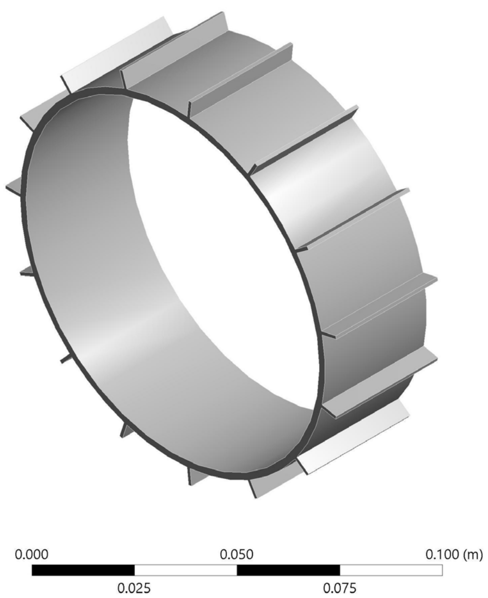

Figure 6: Axial fin CATIA model.

Figure 7: Radial fin CATIA model.

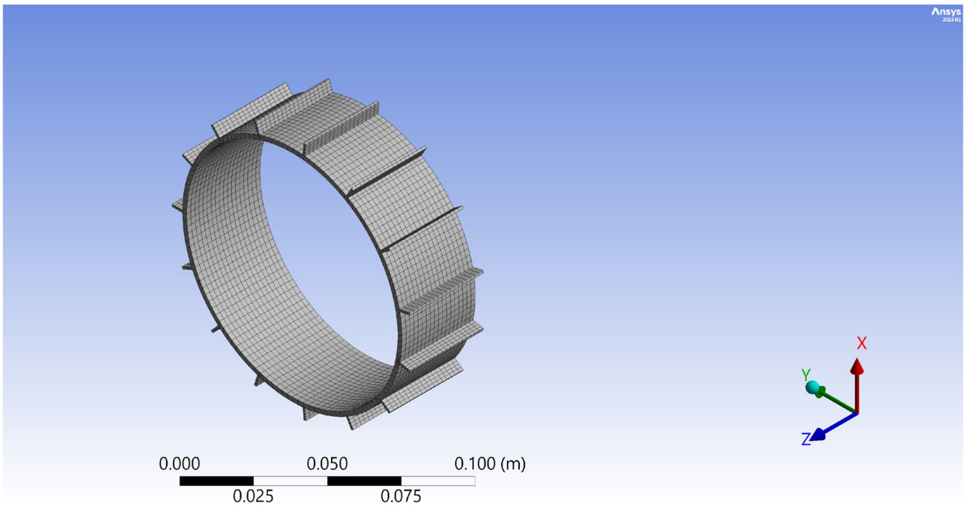

Figure 8: Mesh of axial fin.

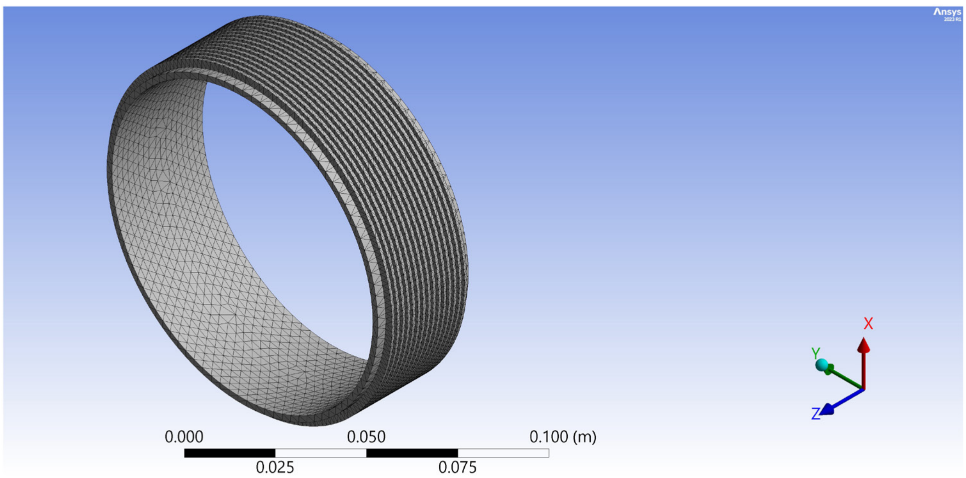

Figure 9: Mesh of radial fin.

5. STEADY-STATE THERMAL ANALYSIS OF FINS

The SRM case is fitted with axial and radial rectangular fins. This fin arrangement improved the surface area of contact for heat dissipation. The ANSYS solver is run to get the numerical results. The average fin tip temperature is taken as output to compare the different geometry models. Figure 10 shows the temperature distribution of the radial fins made of Al/Diamond MMC material. Figure 11 shows the temperature distribution of the electric motor case with axial fins made of Al/Diamond MMC material. Figure 12 shows the average fin tip temperature of the different Al/MMC. The fin made with Al/Diamond MMC fin has the minimal tip temperature for both radial and axial fins. Since this material has very high thermal conductivity when compared to the other two MMC materials. So, for further analysis the Al/Diamond MMC material is utilized. The steady-state thermal analysis of MSRSRM is conducted to identify the effective heat generation and distribution. The external fins are placed in the stator of the motor for proper thermal management. The steady state thermal analysis of fins is carried to identify the type fins, thickness, and effective number of fins. Through the steady state analysis itself, the important parameters such as temperature distribution, heat transfer rate, types of fins and the effectiveness of fin geometry can be easily determined.

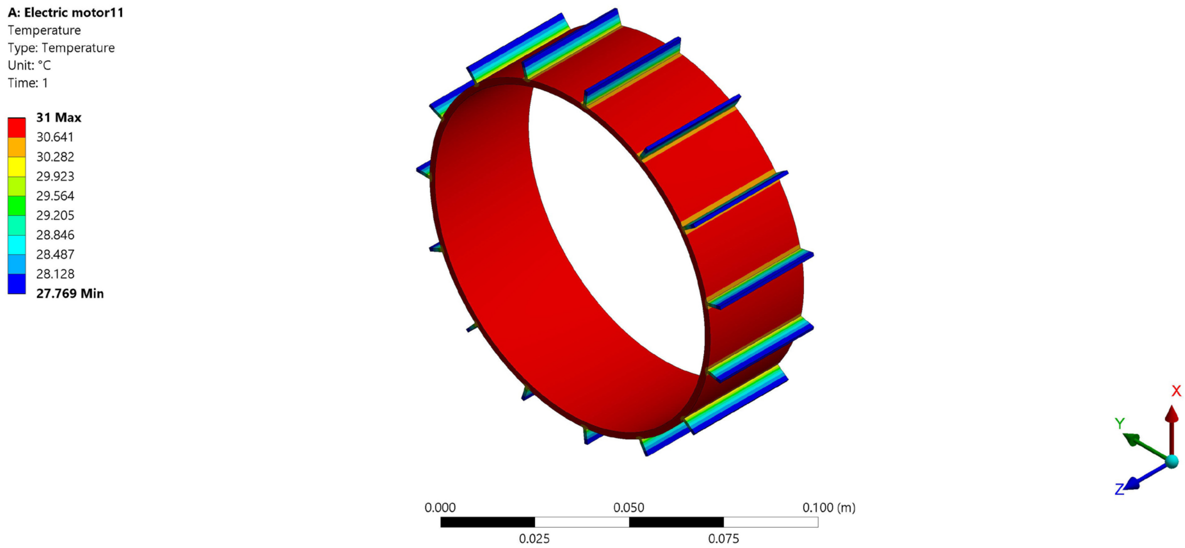

Figure 10: Temperature distribution of radial fins made of Al/Diamond MMC material.

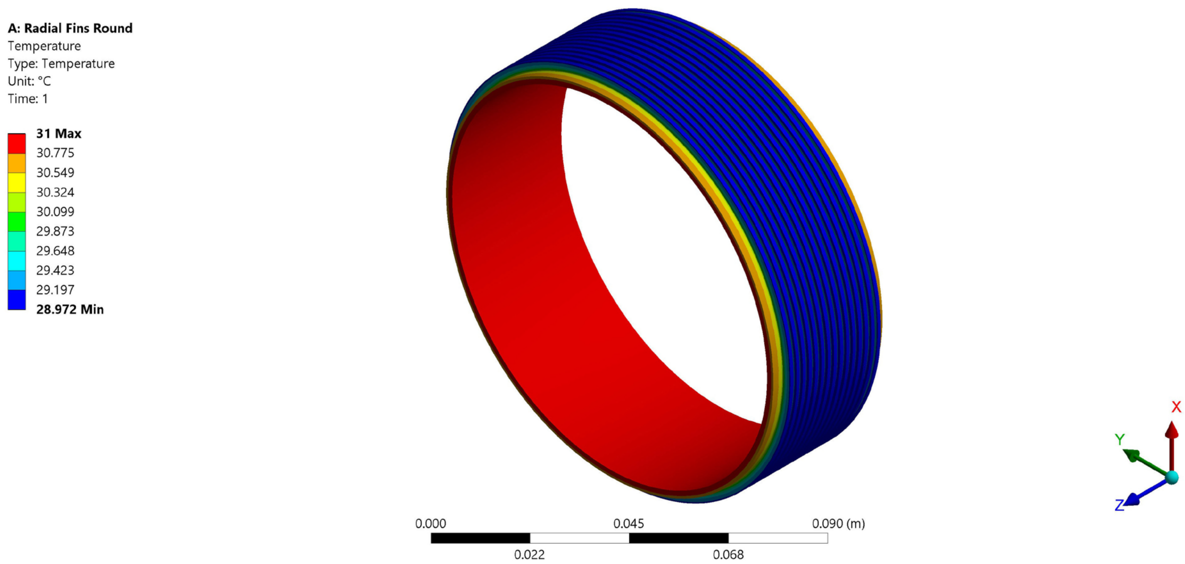

Figure 11: Temperature distribution of axial fins made of Al/Diamond MMC material.

The Al/Diamond MMC has higher thermal conductivity compare with other two materials. Through numerical analysis, it is evident that the Al/Diamond MMC fins has least fin tip temperature (Figure 10). Due to the good thermal conductivity and moderate specific heat properties, the Al/Diamond MMC can absorb more heat per unit mass without experiencing the significant rise in the temperature when compared with other two materials. From the results, it is evident that the Al/Diamond MMC material is more suited for fins of the MSRSRM. The numerical analysis is carried out for fins with all the three proposed materials. Table 5 represents the numerical results obtained through finite element study. From the results, it is identified Al/Diamond MMC yields better results. Further thermal analysis of the fins is carried out based on the Al/Diamond MMC material and the corresponding results are included.

After chosen the material, the effect of fin count and gap between the fins must be analysed. The fin count is varied as 5, 10 and 15 for further numerical analysis. The numerical analysis results are used to find the optimum number of fins. The pitch of the fin is varied according to the fin count. The object of this analysis is to find the optimum number of fins for effective waste heat losses to the surroundings. The optimum number of fins on the SRM gives maximum heat transfer on minimum fin count. Thus, the overall mass of the fin is reduced. The steady state thermal analysis of axial direction and radial direction fin are analysed in this work.

Figure 13 shows the temperature at the fin tip for the radial fin arrangement. Figure 14 shows the temperature at the fin tip for the axial fin arrangement. The minimum temperature at the fin tip is found to be 27.769°C for axial fin and 28.972°C for radial fin arrangement respectively. Figure 15 shows the mass of the axial fin arrangement and Figure 16 shows the mass of the radial fin arrangement. As the fin count increases, the overall mass of the fin increases and the fin tip temperature decreases. The maximum mass of the fin is found to be 2.5 Kg for the axial fin and 3.36 Kg for the radial fin arrangement respectively. The mass of the fin defines the overall weight of the SRM. Generally, thin fins have higher effectiveness compared to thin fins. The mass of the SRM is increased due to the usage of thick fins. The axial fins (15 counts) having a thickness of 1 mm have better results compared to other types of fin arrangements. At this condition, the fin tip temperature is found to be 28.75°C and the mass is found to be 2.0901 Kg.

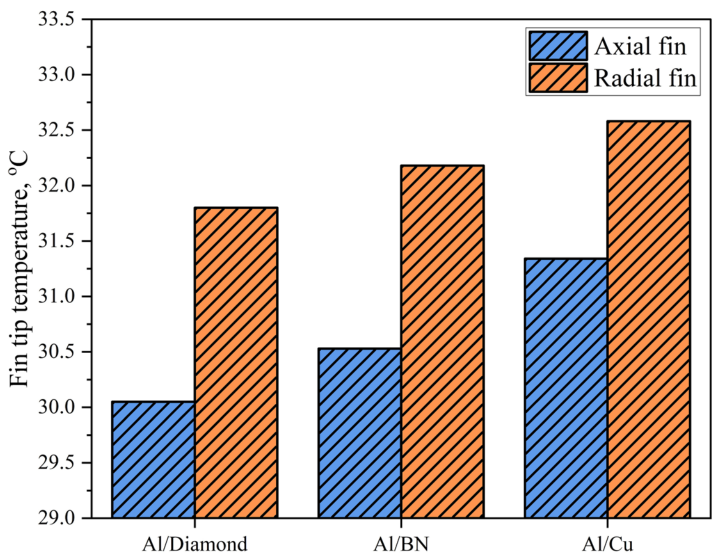

Figure 12: Temperature distribution of axial and radial fins made of Al/MMC material.

Table 5: Average fin tip temperature.

MATERIALS	AVERAGE FIN TIP TEMPERATURE	
	AXIAL FIN	RADIAL FIN
Al/Diamond MMC	30.05°C	31.8°C
Al/BN MMC	30.53°C	32.18°C
Al/Cu MMC	31.34°C	32.58°C

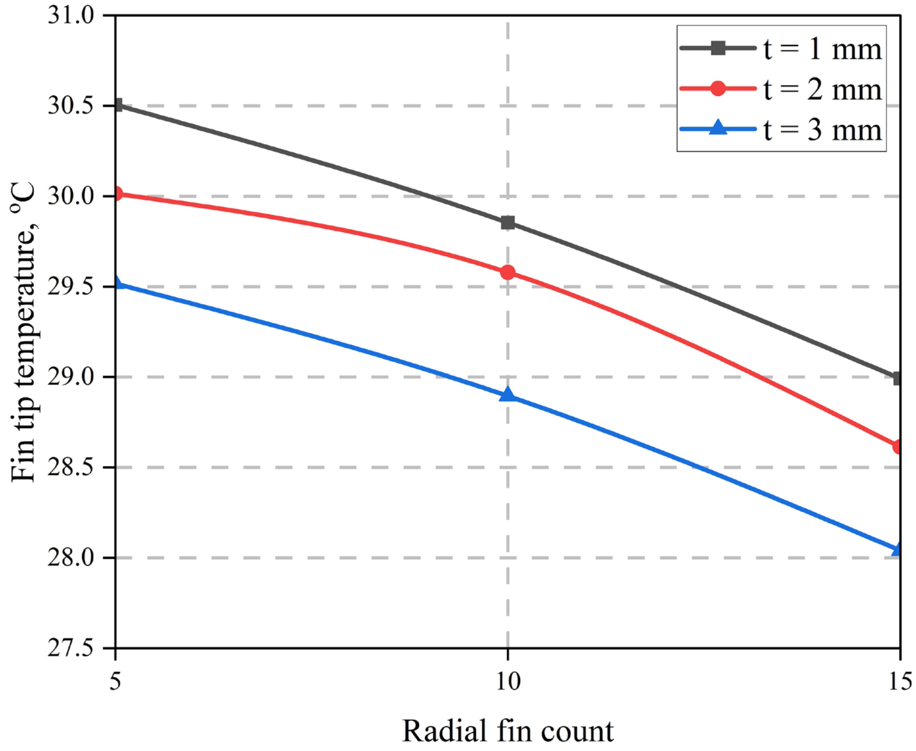

Figure 13: Temperature at the fin tip for the different radial fin count.

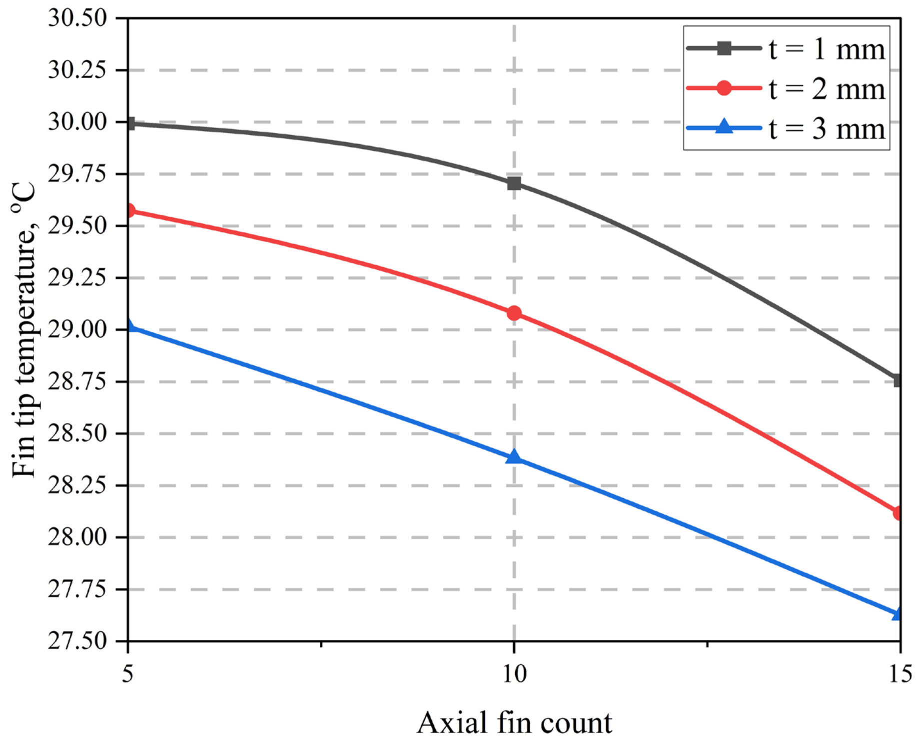

Figure 14: Temperature at the fin tip for the different axial fin count.

6. CONCLUSIONS

The work presented in the manuscript investigated the thermal analysis of MSRSRM with external fin arrangements. Initially, the electromagnetic analysis of the machine is carried out. The results revealed the superiority of the proposed MSRSRM. When compared with other SRM topologies, it yields better torque

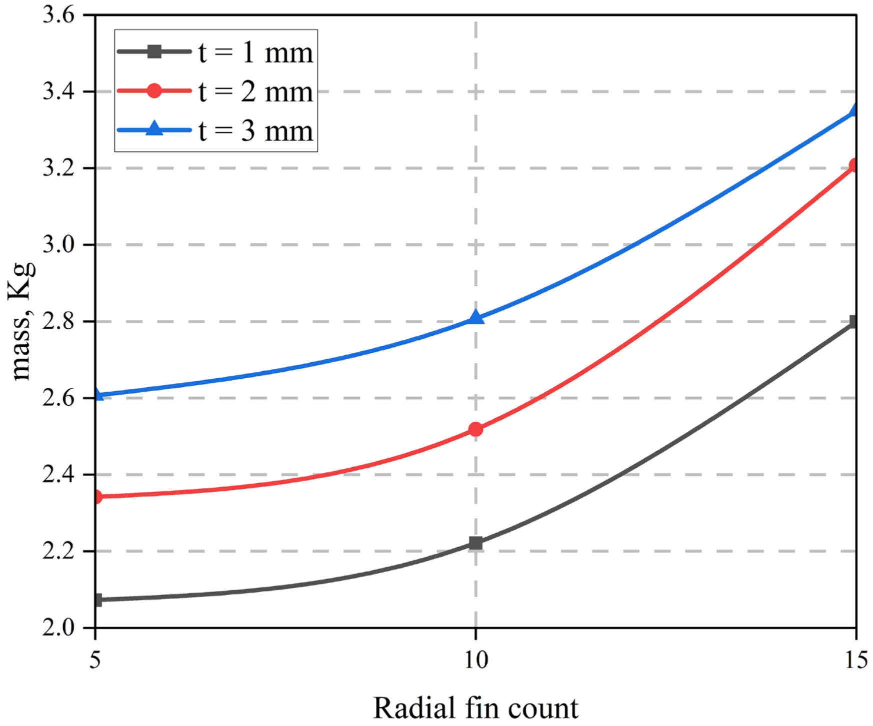

Figure 15: Mass of the axial fin vs fin count.

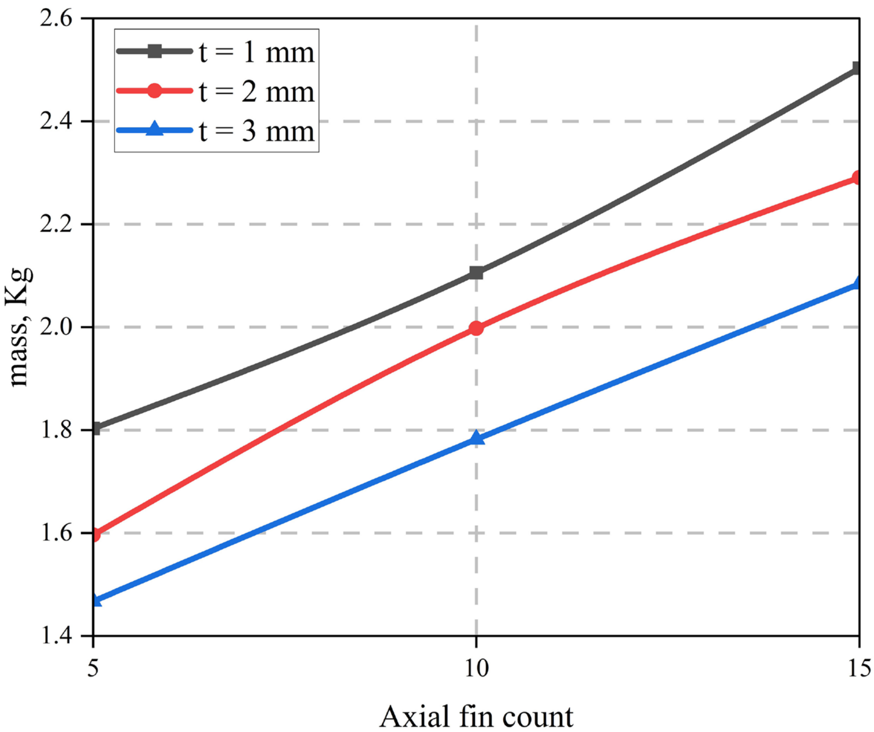

Figure 16: Mass of the radial fin vs fin count.

production with minimum ripples of 1.525 p.u. The steady-state and transient thermal analysis of the MSRSRM is further carried out to identify the temperature distribution of the machine. From the obtained results, it is identified that the temperature rise in the stator and rotor of the MSRSRM is higher than the conventional SRM. For effective thermal management of the MSRSRM, the external fins are provided in the stator of the machine. There are three Al MMC fin materials are chosen for the numerical analysis of the present study. Among the three materials chosen, the Al/Diamond MMC has higher thermal conductivity and yields better results. When compared with Al/Cu and Al/BN MMC, the Al/Diamond fins have minimum fin temperature. Further, the analysis is extended to identify the suitable type of fin configuration (axial or radial), the thickness of the fins, and the optimum number of fins. From the results, it is proven that the axial type Al/Diamond thin fins size in 1 mm are found to be better when compared with other configurations. The work can be further extended to real-time hardware implementation of cooling fan applications.

7. BIBLIOGRAPHY

[1] KONDELAJI, M.A.J., MIRSALIM, M., "Segmented-rotor modular switched reluctance motor with high torque and low torque ripple", *IEEE Transactions on Transportation Electrification*, v. 6, n. 1, pp. 62–72, 2020. doi: http://doi.org/10.1109/TTE.2020.2969356.

[2] RAJ, E., APPADURAI, M., RANI, E., *et al.*, "Finite-element design and analysis of switched reluctance motor for automobile applications", *Multiscale and Multidisciplinary Modeling, Experiments and Design*, v. 5, n. 3, pp. 269–277, 2022. doi: https://doi.org/10.1007/s41939-022-00119-8.

[3] SIJINI, A.C., FANTIN, E., RANJIT, L.P., "Switched reluctance motor for hybrid electric vehicle", *Middle East Journal of Scientific Research*, v. 24, n. 3, pp. 734–739, 2016.

[4] RAMANA, G.V., MUNI, T.V., SUBBARAYUDU, C.B.V., *et al.*, "Improving the maximum power point tracking in wind farms with PID and artificial intelligence controllers for switched reluctance generators", In *2022 International Conference on Futuristic Technologies (INCOFT),* pp. 1–6, Belgaum, India, Nov. 2022. doi: http://doi.org/10.1109/INCOFT55651.2022.10094347.

[5] MEHTA, S., KABIR, M.A., PRAMOD, P., *et al.*, "Segmented rotor mutually coupled switched reluctance machine for low torque ripple applications", *IEEE Transactions on Industry Applications*, v. 57, n. 4, pp. 3582–3594, 2021. doi: http://doi.org/10.1109/TIA.2021.3073384.

[6] ZHANG, H., LEE, D.H., AHN, J.W., "Design and analysis of segmented rotor Type 12/8 switched reluctance motor", *Journal of Power Electronics*, v. 14, n. 5, pp. 866–873, 2014. doi: http://doi.org/10.6113/JPE.2014.14.5.866.

[7] RAJ, E.F.I., KAMARAJ, V., "Neural network based control for switched reluctance motor drive", In: *2013 IEEE international conference on emerging trends in computing, communication and nanotechnology (ICECCN),* pp. 678–682, Tirunelveli, India, March 2013. doi: http://doi.org/10.1109/ICE-CCN.2013.6528586.

[8] XU, Z., LEE, D.H., AHN, J.W., "Design and operation characteristics of a novel switched reluctance motor with a segmental rotor", *IEEE Transactions on Industry Applications*, v. 52, n. 3, pp. 2564–2572, 2016. doi: http://doi.org/10.1109/TIA.2016.2519858.

[9] XU, Z., LEE, D.H., AHN, J.W., "Design and operation characteristics of a novel switched reluctance motor with a segmental rotor", *IEEE Transactions on Industry Applications*, v. 52, n. 3, pp. 2564–2572, 2016. doi: http://doi.org/10.1109/TIA.2016.2519858.

[10] SUN, W., LI, Q., LIU, K., *et al.*, "Design and analysis of a novel rotor-segmented axial-field switched reluctance machine", *CES Transactions on Electrical Machines and Systems*, v. 1, n. 3, pp. 238–245, 2017. doi: http://doi.org/10.23919/TEMS.2017.8086102.

[11] ZENG, L., YU, H., "Research on a novel rotor structure switched reluctance motor", *Physics Procedia*, v. 24, pp. 320–327, 2012.

[12] BALAJI, M., RAMKUMAR, S., KAMARAJ, V., "Sensitivity analysis of geometrical parameters of a switched reluctance motor with modified pole shapes", *Journal of Electrical Engineering & Technology*, v. 9, n. 1, pp. 136–142, 2014. doi: http://doi.org/10.5370/JEET.2014.9.1.136.

[13] GNANIAH, A.M., MAHADEVAN, B., VIJAYARAJAN, K., "Influence of laminating materials and modified pole shapes on the performance of segmented rotor switched reluctance motor", *Journal of Magnetism*, v. 25, n. 3, pp. 347–354, 2020. doi: http://doi.org/10.4283/JMAG.2020.25.3.347.

[14] AUGUSTINE, M., RAJ, E.F.I., APPADURAI, M., *et al.*, "Impact of silicon steel laminating materials in modified segmented rotor switched reluctance motor: electromagnetic and vibrational analysis", *Journal of Vibration Engineering & Technologies*, pp. 1–16, 2023.

[15] FAN, J., ZHANG, C., WANG, Z., *et al.*, "Thermal analysis of permanent magnet motor for the electric vehicle application considering driving duty cycle", *IEEE Transactions on Magnetics*, v. 46, n. 6, pp. 2493–2496, 2010. doi: http://doi.org/10.1109/TMAG.2010.2042043.

[16] JALALI, H., "Thermal analysis of Double Stator Switched Reluctance Machine (DSSRM) using finite element method", *Journal of Electrical Engineering*, v. 16, n. 3, pp. 7–7, 2016.

[17] YAN, W., CHEN, H., LIU, Y., *et al*., "Iron loss and temperature analysis of switched reluctance motor for electric vehicles", *IET Electric Power Applications*, v. 14, n. 11, pp. 2119–2127, 2020. doi: http://doi.org/10.1049/iet-epa.2020.0166.

[18] LI, S., ZHANG, S., HABETLER, T.G., *et al*., "Modeling, design optimization, and applications of switched reluctance machines—A review", *IEEE Transactions on Industry Applications*, v. 55, n. 3, pp. 2660–2681, 2019. doi: http://doi.org/10.1109/TIA.2019.2897965.

[19] FANTIN IRUDAYA RAJ, E., BALAJI, M., "Analysis and classification of faults in switched reluctance motors using deep learning neural networks", *Arabian Journal for Science and Engineering*, v. 46, n. 2, pp. 1313–1332, 2021. doi: http://doi.org/10.1007/s13369-020-05051-y.

[20] FAIZ, J., IRANPOUR, R., PILLAY, P., "Thermal model for a switched reluctance motor of TEFC design during steady and transient operation," *Electric Machines and Power Systems*, v. 26, no. 1, pp. 77–91, 1998. doi: http://doi.org/10.1080/07313569808955809.

[21] SUNDARAMOORTHY, P., MAHADEVAN, B., "Analysis and implementation of two phase flux reversal free doubly salient machine", *Journal of Magnetics*, v. 23, n. 3, pp. 350–359, 2018. doi: http://doi.org/10.4283/JMAG.2018.23.3.350.

[22] AUGUSTINE, M., BALAJI, M., KAMARAJ, V., "Characteristics assessment of switched reluctance motor with segmented rotor", In *2019 IEEE 1st International Conference on Energy, Systems and Information Processing (ICESIP),* pp. 1–6, Chennai, India, July 2019. doi: http://doi.org/10.1109/ICESIP46348.2019.8938386.

[23] FANTIN IRUDAYA RAJ, E., APPADURAI, M., "Static 2D-finite element analysis of eccentricity fault in induction motor", In: *Smart Technologies for Energy, Environment and Sustainable Development, Vol 1: Select Proceedings of ICSTEESD 2020*, pp. 409–422, Singapore, Springer Nature, 2022. doi: http://doi.org/10.1007/978-981-16-6875-3_33.

[24] APPADURAI, M., RAJ, E.F.I., VENKADESHWARAN, K., "Finite element design and thermal analysis of an induction motor used for a hydraulic pumping system", *Materials Today: Proceedings*, v. 45, pp. 7100–7106, 2021. http://doi.org/10.1016/j.matpr.2021.01.944.

[25] İRIZALP, A.O., DURMUŞ, H., YÜKSEL, N., *et al*., "Cold metal transfer welding of AA1050 aluminum thin sheets", *Matéria (Rio de Janeiro)*, v. 21, pp. 615–622, 2016. doi: https://doi.org/10.1590/S1517-707620160003.0059.

[26] GOVINDAN, K., RAGHUVARAN, J.G., "Mechanical properties and metallurgical characterization of LM25/ZrO2 composites fabricated by stir casting method", *Matéria (Rio de Janeiro)*, v. 24, n. 3, pp. e12439, 2019. http://doi.org/10.1590/s1517-707620190003.0753.

[27] BENCOMO, A., BISBAL, R., MORALES, R., "Simulation of the aluminum alloy A356 solidification cast in cylindrical permanent molds", *Matéria (Rio de Janeiro)*, v. 13, pp. 294–303, 2008. doi: https://doi.org/10.1590/S1517-70762008000200007.

[28] BUSTOS, Ó., ALLENDE, R., LEIVA, R., *et al*., "Effect of magnetic stirring, grain modification and refinement on the solidification structure of an A356 aluminum alloy", *Matéria (Rio de Janeiro)*, v. 26, n. 1, pp. e12927, 2021. doi: http://doi.org/10.1590/s1517-707620210001.1227.

[29] DINIZ, S.B., PAULA, A.D.S., BRANDÃO, L.P., "Temperature and annealing time influences on cross-rolled 7475-T7351 aluminum alloy", *Matéria (Rio de Janeiro)*, v. 27, n. 4, pp. e20220167, 2022. doi: http://doi.org/10.1590/1517-7076-rmat-2022-0167.

[30] BERLIN PUSH, P.R., BAVANISH, B.R., "Experimental investigation on the mechanical properties of Al2024 doped with green synthesized quantum dots", *Matéria (Rio de Janeiro)*, v. 28, n. 4, pp. e20230200, 2024. doi: http://doi.org/10.1590/1517-7076-rmat-2023-0200.

[31] MASOUMI, M., JALALI KONDELAJI, M.A., MIRSALIM, M., *et al*., "Analytical modelling and experimental verification of E-type reluctance motors", *IET Electric Power Applications*, v. 13, n. 1, pp. 110–118, 2019. doi: http://doi.org/10.1049/iet-epa.2018.5421.

[32] FANTIN IRUDAYA RAJ, E., APPADURAI, M., "Minimization of torque ripple and incremental of power factor in switched reluctance motor drive", In: Pundir, A. K. S., Yadav, A., Das, S. (eds), *Recent trends in communication and intelligent systems*, Singapore, Springer, pp. 125–133, 2021. doi: http://doi.org/10.1007/978-981-16-0167-5_14.

[33] KRISHNAN, R., *Switched reluctance motor drives: modeling, simulation, analysis, design, and applications*, Boca Raton, CRC Press, 2017. doi: http://doi.org/10.1201/9781420041644.

[34] LUO, J., KHATTINEJAD, R., ASSARI, A., *et al*., "Microstructure, mechanical and thermal properties of Al/Cu/SiC laminated composites, fabricated by the ARB and CARB processes", *Crystals*, v. 13, n. 2, pp. 354, 2023. doi: http://doi.org/10.3390/cryst13020354.

[35] WANG, P.P., CHEN, G.Q., LI, W.J., *et al*., "Microstructural evolution and thermal conductivity of diamond/Al composites during thermal cycling", *International Journal of Minerals Metallurgy and Materials*, v. 28, n. 11, pp. 1821–1827, 2021. doi: http://doi.org/10.1007/s12613-020-2114-0.

[36] CHEN, C., GUO, L., LUO, J., *et al*., "Aluminum powder size and microstructure effects on properties of boron nitride reinforced aluminum matrix composites fabricated by semi-solid powder metallurgy", *Materials Science and Engineering A*, v. 646, pp. 306–314, 2015. doi: http://doi.org/10.1016/j.msea.2015.08.081.